Tropical Cyclones and Transient Upper-Ocean Warming

CLAUDIA PASQUERO

Earth System Science Department, University of California, Irvine, Irvine, California

KERRY EMANUEL

Program in Atmospheres, Oceans, and Climate, Massachusetts Institute of Technology, Cambridge, Massachusetts

(Manuscript received 20 June 2006, in final form 25 April 2007)

ABSTRACT

Strong winds affect mixing and heat distribution in the upper ocean. In turn, upper-ocean heat content affects the evolution of tropical cyclones. Here the authors explore the global effects of the interplay between tropical cyclones and upper-ocean heat content. The modeling study suggests that, for given atmospheric thermodynamic conditions, regimes characterized by intense (with deep mixing and large upper-ocean heat content) and by weak (with shallow mixing and small heat content) tropical cyclone activity can be sustained. A global general circulation ocean model is used to study the transient evolution of a heat anomaly that develops following the strong mixing induced by the passage of a tropical cyclone. The results suggest that at least one-third of the anomaly remains in the tropical region for more than one year. A simple atmosphere–ocean model is then used to study the sensitivity of maximum wind speed in a cyclone to the oceanic vertical temperature profile. The feedback between cyclone activity and upper-ocean heat content amplifies the sensitivity of modeled cyclone power dissipation to atmospheric thermodynamic conditions.

1. Introduction

The current understanding of tropical cyclone thermodynamics predicts a dependence of its thermodynamic potential intensity (PI) on the sea surface temperature (Emanuel 2003). The amount of energy dissipated in the boundary layer by turbulence is ultimately balanced by energy extracted from the ocean through evaporation of seawater. Higher sea surface temperature (SST) allows for a higher rate of energy transfer from the ocean, and so for a larger PI. In most cases, the actual intensity of a tropical cyclone differs from the potential intensity, as other factors not included in the thermodynamic balance come into play, including vertical shear of horizontal winds, mixing of eyewall air with its environment, and ocean interactions (Emanuel et al. 2004; Persing and Montgomery 2003). Assuming that, on average, the ratio between the actual wind speeds in tropical cyclones and their potential intensity is constant, Emanuel (1987) predicted a small increase in tropical cyclone power with increased SST, of the order of 10% for a 0.5°C warming of the sea surface. Similar estimates have been obtained using more sophisticated models (Knutson and Tuleya 2004; Knutson et al. 2001). Those estimates, however, pertain to large-scale temporal increases of SST and are not representative of the sensitivity that tropical cyclones have to localized spatial variations of SST: a relatively small decrease in the SST gradient between the eye of a tropical cyclone and the surrounding water is able to significantly increase the maximum wind speed (Emanuel 2007; Schade 2000). Sea surface temperatures and power dissipated by cyclones over the last few decades are indeed correlated (Elsner et al. 2006; Emanuel 2005), but the magnitude of the variations is surprising. The observed variation in the power dissipated by tropical cyclones is on the order 70%, for large-scale temporal changes in SST of 0.5°C. Although the correlation between the two signals could be inconsequential and given that we want to understand the mechanisms that create variations in tropical cyclone activity, we use the observed correlation as suggestive of a direct linkage between SST and tropical cyclone activity. In this

Corresponding author address: Claudia Pasquero, Earth System Science Department, University of California, Irvine, Irvine, CA 92697-3100.
E-mail: claudia.pasquero@uci.edu

DOI: 10.1175/2007JCLI1550.1

© 2008 American Meteorological Society

case, the disparity between the predicted and the observed sensitivity of tropical cyclone activity to the changes in sea surface temperature needs to be addressed. We suggest that the distribution of the ratio between the observed maximum tropical cyclone intensity and the PI is not constant but rather depends on the ocean heat content, which is in turn affected by tropical cyclone activity, as briefly summarized below.

The passage of tropical cyclones leaves a wake on the ocean surface, encompassing water that is cooled by up to several degrees Celsius (Bender et al. 1993; Cione and Uhlhorn 2003). Most of this cooling is associated with entrainment of colder water upwelled by strong winds, rather than by air–sea heat loss (D'Asaro 2003; Price 1981). Large wind stress creates strong velocity shear in the upper ocean. Shear instabilities deepen the mixed layer, generating surface cooling and subsurface warming (Emanuel 2001). The SST is subsequently restored to typical values by oceanic processes and anomalous air–sea heat fluxes (e.g., reduced latent heat loss), entailing a net positive heat flux into the ocean. This net heating is associated with a warming that is located away from the surface, in the region at the base of the mixed layer. Emanuel (2001) estimated for the year 1996 a total heat flux of $(1.4 \pm 0.7)\ 10^{15}$ W into the ocean induced by global tropical cyclone activity. In steady-state annual mean conditions, such heat is eventually transported away by ocean currents, and most likely lost to the atmosphere at different latitudes.

In this paper, we focus on the fate of subsurface warm anomalies created by an anomalously strong tropical cyclone season and speculate about the possible implications of transient heat anomalies in the upper ocean on subsequent tropical cyclone events. A positive feedback between strong cyclones and warm anomalies at the base of the mixed layer is potentially at play. There is evidence that, when a tropical cyclone passes over a warm ring characterized by a deep mixed layer and correspondingly large heat content, its intensity rapidly increases (D'Asaro 2003; Goni and Trinanes 2003; Lin et al. 2005; Shay et al. 2000). Goni and Trinanes (2003) find that "the intensification of 32 out of the 36 strongest tropical cyclones in the tropical Atlantic, from 1993 to 2000, [. . .] can be associated with the passage of their tracks over regions with increased heat potential of at least 20 kJ/cm^2." In most cases, the heat anomaly is not reflected in higher sea surface temperature, indicating that the subsurface heat is an important quantity in tropical cyclone intensity prediction (Goni and Trinanes 2003). Cooling of the sea surface by entrainment of colder water is one of the processes that inhibit hurricane intensification, preventing them from reaching their PI (Bender and Ginis 2000; Bender et al. 1993; Emanuel 1999; Knutson et al. 2001; Schade 2000; Zhu and Zhang 2006). This has been referred to as the SST feedback mechanism (Schade and Emanuel 1999).

The hypothesis that we here present and test is that, as tropical cyclone intensity and duration increase, there is more entrainment and a transient deep mixed layer is formed. The relaxation of SST to typical conditions will be associated with anomalous heating of the subsurface ocean. The resulting extra heat in the water column will reduce the negative SST feedback on tropical cyclones subsequently passing over the same area. Clearly, for this mechanism (discussed in section 2) to be important, the anomalous heating must be sufficiently large and the dissipation time of the heat anomaly at the base of the mixed layer must be longer than the time interval between the passage of tropical cyclones. We here use an ocean general circulation model to estimate the lifetime and the amplitude of such heat anomalies (section 3). We then use a coupled hurricane–ocean model to estimate the effect of these anomalies on tropical cyclone intensity (section 4). In section 5, we use a simple model to calculate the evolution of the anomalies over time scales of several years. The results are summarized and discussed in section 6, in relation to observational oceanographic data of the last few decades.

2. The feedback mechanism

The potential intensity of a tropical cyclone is defined as the maximum attainable wind speed, considering the cyclone as a thermodynamic engine. Its dependence on the environmental characteristics is (Emanuel 2003)

$$|V_p|^2 = \frac{C_k}{C_D}\frac{T_s - T_o}{T_o}(k_0^* - k), \tag{1}$$

where C_D and C_k are the air–sea momentum and heat exchange coefficients, respectively, T_s is the air temperature at the ocean surface, T_o is the entropy-weighted mean outflow temperature at the top of the storm, k is the specific enthalpy of air in the boundary layer at temperature T_s, and k_0^* is the specific enthalpy of saturated air at temperature T_s. The difference between T_s and T_o has fairly small variability over different climatic conditions, and it is not expected to change significantly in a warmer world. Similarly, the air–sea momentum exchange coefficient C_D and the heat exchange coefficient C_k are usually considered independent of temperature. The expected climate sensitivity of V_p is derived from consideration of the energy bal-

ance at the ocean surface. Enough thermodynamic disequilibrium, $(k_0^* - k)$, must be present to maintain the turbulent enthalpy flux required to balance the net radiative flux at the surface. An increase in the latter (induced, for instance, by increased greenhouse gases) requires an increase in thermodynamic disequilibrium, provided there is no change in the mean surface wind speed. Such reasoning predicts a few percent change in the wind speed of tropical cyclones when SST changes by 0.5°C (Emanuel 2005; Knutson and Tuleya 2004). This small sensitivity is consistent with the findings of Michaels et al. (2006) who observed that the ultimate intensity that a storm achieves is less dependent on the underlying SST than it is on many other environmental factors. Considering that the total power dissipated in the boundary layer depends on the time integral of the third power of wind speed and that storm duration also generally increases with intensity, a larger sensitivity is expected (resulting in, at most, a 20% increase in dissipated power per SST warming of 0.5°C), but certainly not as large as observed (about 70%). The idea behind this reasoning is that $\mathrm{PD} = \mathcal{F} V_p^3$, with $\mathcal{F}$ a proportionality factor that scales as $\phi C_D \rho L^2 T$, where ρ is the density of water, L and T are spatial and temporal scales of tropical cyclones, respectively, and ϕ is a coefficient smaller than one that represents the fact that usually the power dissipated by tropical cyclones is smaller than the thermodynamic potential value, $\mathrm{PPD} = C_D \rho L^2 T V_p^3$ (Emanuel 2000). We thus have

$$\mathrm{PD} = \phi \mathrm{PPD}. \tag{2}$$

The proportionality factor ϕ depends on many factors, including vertical shear of the horizontal winds and interactions with land and ocean. We here focus on its dependence on the upper-ocean heat content (HC) that, in turn, is a function of the stirring in the upper ocean, and thus of the power dissipated (PD) by preceding tropical cyclones. The feedback between PD and HC is the subject of this work.

Indicating reference conditions with a subscript, X_0, we construct the following toy model for the upper-ocean heat content evolution:

$$\frac{d\mathrm{HC}}{dt} = \frac{1}{\tau}(\mathrm{HC}_0 - \mathrm{HC}) + \gamma \frac{\mathrm{PD} - \mathrm{PD}_0}{\mathrm{PD}_0}. \tag{3}$$

The evolution equation for the upper-ocean HC has a relaxation term to unperturbed steady-state conditions HC_0 that acts on a time-scale τ and a forcing term that depends on the anomalous power dissipated by tropical cyclones in the upper ocean. The factor γ is the heat flux into the ocean associated with normal tropical cyclone activity. If $\mathrm{PD} = \mathrm{PD}_0$, there is no heating anomaly. Defining the heat anomaly, $\xi = (\mathrm{HC} - \mathrm{HC}_0)$ and substituting $\mathrm{PD} = \phi(\xi)\,\mathrm{PPD}$ (potential power dissipated) in the equation above, we obtain

$$\frac{d\xi}{dt} = \gamma\left(\frac{\phi(\xi)}{\phi(0)}\frac{\mathrm{PPD}}{\mathrm{PPD}_0} - 1\right) - \frac{1}{\tau}\xi. \tag{4}$$

In the following, we evaluate the different parameters so as to obtain an estimate for how important the different terms in the above equation are. We next describe simulations with the Massachusetts Institute of Technology general circulation model (MITgcm) that allow us to estimate reasonable values for γ and τ. The dependence of ϕ on the heat content anomaly will be estimated with the use of a hurricane model coupled to a simple ocean model.

3. Ocean model

Here we study the transient response of an ocean model to a perturbation designed to represent the upper-ocean mixing created by anomalously strong tropical cyclones. To this end, we use the MITgcm (Marshall et al. 1997), run under annual mean forcing, on a horizontal grid of $4° \times 4°$ with 20 geopotential vertical levels and a higher resolution in the upper ocean (5 layers in the first 200 m). The model is driven using annual mean winds, Haney-type mixed boundary conditions for surface temperature, and fixed freshwater flux. All boundary conditions are time independent and represent annual mean properties. There are no explicit mixed layer dynamics: the first layer, interpreted as a mixed layer, has a prescribed thickness of 50 m (below it, the vertical resolution becomes 25 m). After a spinup of 1000 years, the model reaches a steady state (small fluctuations in the model variables are still present, but they are negligible for our study). The flow in the upper layer is shown in Fig. 1. This is our control state.

We then add a perturbation in the temperature field that is meant to represent the effects of enhanced tropical cyclone activity: in the geographical regions over which the estimated annual mean PI is large ($\mathrm{PI} > 60$ m s^{-1}, see Fig. 2) and outside an equatorial band of 8° latitude width, the surface water is mixed down to 75 m, that is, one grid level below the 50-m-deep model mixed layer. To consider whether this is a realistic perturbation, consider that a typical cold wake after the passage of a tropical cyclone can be 300 km wide and 2000 km long. When multiplying its surface area by the number of tropical cyclones in a year (about 90), we obtain the total area affected by mixing induced by tropical cyclones in a year to be about 50×10^6 km^2, which is only a bit smaller than the surface area of the perturbed region in our simulations (70×10^6 km^2). In the model, surface water is cooled by mixing with sub–mixed layer

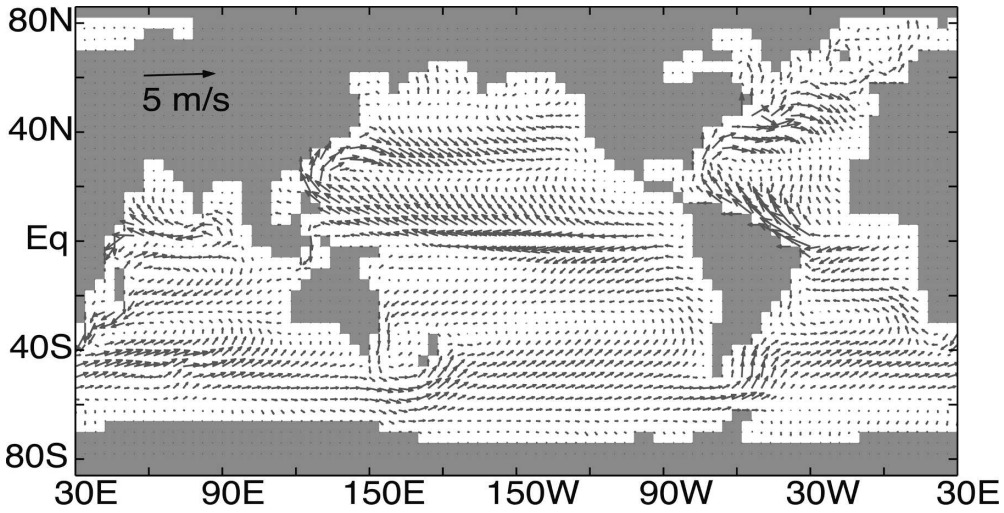

FIG. 1. Surface velocities (25 m) from the MITgcm simulation with annual mean forcing, 4° × 4° resolution, and 20 vertical levels.

water (Fig. 3), resulting in a mean sea surface temperature decrease of 0.72°C over the perturbed area. Note that the specific patterns of those anomalies is different from the pattern that is observed when the mixing procedure is applied to observational climatological dataset (not shown), as the vertical profiles of temperature in the model do not perfectly reproduce the observed ones. It is reassuring, however, that the mean sea surface temperature reduction in the two cases is very similar (0.72°C in our model and 0.78°C in the World Ocean Atlas dataset). The total heat loss in the mixed layer over the perturbed region due to mixing with colder water integrates to 1.1×10^{22} J. To put this in perspective, consider that Emanuel (2001) estimated the energy change in the upper ocean due to the mixing with underlying colder water, integrated over 1 year of tropical cyclone activity, to be $4.5 \times 10^{22} \pm 50\%$ J. The main difference is probably due to an underestimate of the mixing depth in our simulation. This implies that we are probably underrepresenting the global effect of tropical cyclone activity on ocean mixing. On the issue of uniform mixing (introduced in our simulations) versus space and time localized mixing (typical of tropical cyclone activity), the reader is referred to Boos et al. (2004) and Scott and Marotzke (2002).

After the perturbation is added, sea surface temperatures relax back to typical values over a characteristic time scale of about two months. During the first months after the perturbation, the air–sea fluxes over the per-

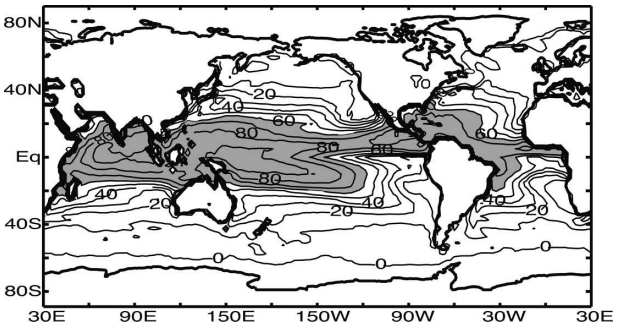

FIG. 2. Maximum sustainable surface wind ($m\,s^{-1}$) calculated from climatological SST data (Conkright et al. 2002) and from reanalysis of vertical profiles of atmospheric temperature, pressure, and mixing ratio. The estimate corresponds to 80% of the maximum gradient wind speed, calculated following the procedure described in Bister and Emanuel 2002. Shaded area corresponds to regions where PI exceeds 60 $m\,s^{-1}$. For the rest of the paper, this area is interpolated onto a 4° × 4° grid by requiring that more than 50% of the 4° × 4° grid cell area have PI > 60 $m\,s^{-1}$.

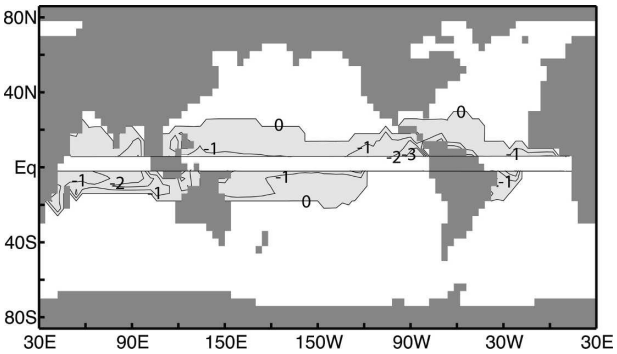

FIG. 3. Surface temperature anomalies (°C) resulting from the mixing of the surface water down to 75 m. Perturbations are only applied to the regions with PI > 60 $m\,s^{-1}$, indicated by the gray contour.

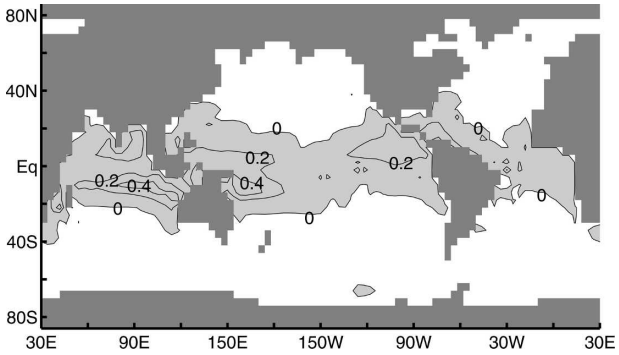

FIG. 4. Subsurface (50–75 m) temperature anomaly 12 months after perturbations were added (°C).

turbed region change in such a way as to reduce the anomalies. After one year, the SST anomalies have been reduced to a mean value of 0.001°C, indicating that the perturbation signature at the surface is almost entirely gone.

What happens below the surface? The temperature anomalies after one year are shown in Fig. 4 for the layer between 50 and 75 m below the surface. These temperatures have peak positive anomalies of 0.5°C. After 12 months, 90% of the anomalous heat is contained between 50 and 155 m below the surface. The heat anomaly evolution over this layer is shown in Fig. 5a. When the initial perturbation is added, an average of 19 kJ cm^{-2} is displaced downward as a result of the mixing with the surface water. This anomaly monotonically decreases as lateral advection and diffusion carry heat away from the water column.

To be more quantitative, we calculate the evolution of the anomalous heat content in the vertical column over the perturbed region. The initial perturbation does not alter the heat content of the column, as heat is simply redistributed in the vertical direction by the anomalous mixing. The evolution of the heat content is a balance between the anomalous heating associated with the relaxation of SST to typical values and the heat flux away from the column that warms surrounding waters. During the first few months after the introduction of the perturbation, anomalous air–sea heat flux is the dominant contribution. This causes a net increase of the column-integrated heat content (see Fig. 5a). After 4–6 months, the SST anomalies have become very weak, and the dominant process is the lateral loss of heat from the deeper layers of the column. This results in a slow decrease of the column-integrated heat content. The decay time scale is about 16 months (Fig. 5b). Values of the initial perturbations and anomalies after 12 months are shown in Table 1. We also indicate the mean anomalous air–sea heat flux, averaged over the first

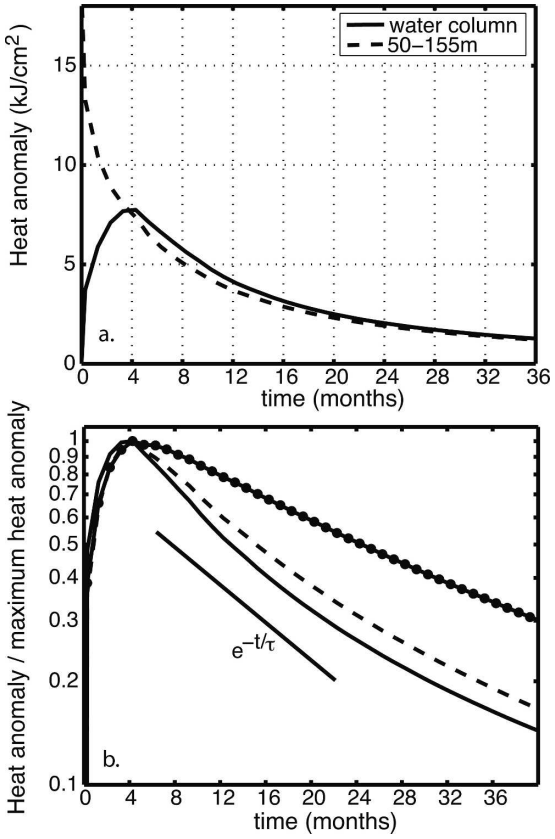

FIG. 5. (a) Evolution of the column-integrated heat anomaly averaged over the perturbed region. Solid line refers to the whole water column; punctuated line is for the layer between 50 and 155 m below the surface. (b) Column-integrated heat anomaly normalized by its maximum value. Solid line is for an initial perturbation down to 75 m, dashed line is for an initial perturbation down to 100 m, and punctuated line is for an initial perturbation down to 155 m. The reference line is an exponential decay with $\tau = 16$ months.

year after the onset of the perturbation and over the whole ocean surface. After a few initial months of anomalous heating, heat is lost as subsurface heat is spread horizontally and vertically. Part of this heat es-

TABLE 1. Anomalous heat content in the water column below the upper 50 m, averaged over the perturbed area, for different initial perturbations. Values indicate the initial perturbation arising from the mixing through the depths indicated in the first column and the anomalies 12 months after. The last column shows the time integral of the anomalous heat flux at the air–sea interface in the first year after the perturbation.

Mixing depths (m)	Initial perturbation (kJ cm^{-2})	Anomaly after 1 yr (kJ cm^{-2})	Anomalous air–sea heat flux integrated over 1 yr (kJ cm^{-2})
0–75	19	4	5.5
0–100	36	10	13
0–155	70	33	38

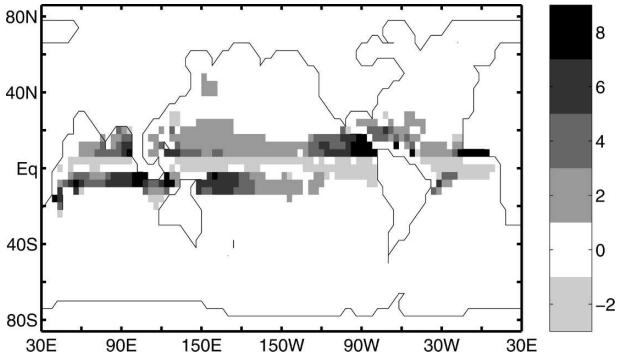

FIG. 6. Surface heat flux anomaly (W m^{-2}) in the first year after the perturbation (W m^{-2}). Red shading indicates anomalous warming; blue shading represents anomalous cooling. The anomalous heat flux, averaged over the perturbed region in the first 12 months from the mixing, is 6×10^{13} W.

capes directly into the atmosphere. Our results indicate that about half of the maximum heat anomaly in the column is lost into the atmosphere without being horizontally advected away.

An exploration of the anomalous heat fluxes at the air–sea interface (Fig. 6) reveals that the ocean mainly gains heat over the perturbed region and loses heat over the equatorial band and near the coasts. The anomalous warm subsurface water in the perturbed area is advected toward lower latitudes over most of the ocean basins, driven by winds. It then upwells in the equatorial area. The resulting warm anomaly is reduced by anomalously large heat loss from the ocean into the atmosphere in the equatorial band. The large-scale circulation is responsible also for heat loss in the western boundary currents where the anomalously large heat loss is visible starting 3 months after the initial mixing, and it reaches its maximum value about 8 months after the perturbation was introduced. This is consistent with the interpretation that the anomaly is carried westward by Rossby waves. The heat loss poleward of the perturbed regions, on eastern boundaries of the basins, is not driven by large-scale advection of warm anomalies over those regions, as here the mean flow is equatorward. It is visible along the west African coast, west Australian coast, and west American coast, and we interpret this as the response to heat transport by Kelvin waves. The small warming visible in the northwest Pacific Ocean and south of New Zealand are present because the ocean model has not reached perfect equilibrium. This small heating does not affect the regions of interest for this study.

We repeated the experiment with two different depths over which the initial mixing is applied: 100 and 155 m. These experiments are performed so as to estimate the sensitivity of the results, and probably they overestimate the global effects of the mixing introduced by tropical cyclone. They are important, however, as intense winds mix water to greater depth than the 75 m used in the first experiment [D'Asaro and McNeil (2007) report a mixing depth of about 150 m after the passage of Hurricane Frances in 2004, which reached category 3]. These simulations indicate that, when the anomalous heat is located at greater depth, the decay time for the anomaly is larger than 16 months (see Fig. 5b). In particular, while after 12 months from the mixing event the heat anomaly in the water column is half of its maximum value for the case of initial mixing down to 75 m, it is as large as 80% of its maximum value when the initial mixing is down to 155 m. For this reason, we think that, by using 16 months as the decay time for the heat anomaly, we are being conservative and that indeed the decay time could be larger. It has to be noted, however, that the simulations presented here do not have mixing with the spatial and temporal intermittency that tropical cyclones have and that the ocean model cannot resolve finescale processes that could be important in the restratification process. More refined studies are needed to better constrain the residence time of anomalous heat in the tropical region and the magnitude of the anomalies.

4. Hurricane–ocean model

Here we use the coupled hurricane–ocean model described in Emanuel et al. (2004) to estimate the dependence of PD on the upper-ocean heat content. The atmospheric component of the model is described in detail by Emanuel (1995). It is constructed on the assumption that the storm is axisymmetric, that the airflow is in hydrostatic and gradient wind balance, and that the vortex is always close to a state of neutral stability to slantwise convection in which the temperature lapse rate is everywhere and always assumed to be moist adiabatic along angular momentum surfaces. Thus the saturated moist potential vorticity is zero everywhere, and the balance conditions allow this quantity to be inverted, subject to certain boundary conditions. These constraints place strong restrictions on the structure of the vortex so that, with the exception of the water vapor distribution, the vertical structure is determined by the radial distribution of boundary layer moist entropy and by the vorticity at the tropopause. The water vapor distribution is characterized by the moist entropy of the boundary layer and of a layer in the middle troposphere. Moist convection is represented by one-dimensional plumes, containing both updrafts and downdrafts, whose mass flux is determined to insure approximate entropy equilibrium of the

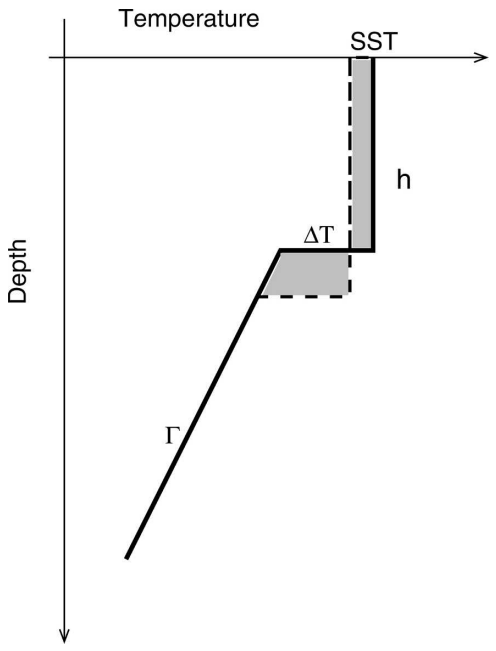

FIG. 7. Schematic representation of the ocean vertical profiles used in the hurricane–ocean model. Dashed line indicates profile after the mixing created by the passage of the hurricane. The two gray regions have the same surface area.

boundary layer. The model variables are phrased in "potential radius" coordinates; potential radius is proportional to the square root of the absolute angular momentum per unit mass about the storm center. This allows for very high radial resolution of the storm's inner core using only a limited number of radial nodes. An empirical parameterization accounts for the effect of environmental wind shear on the storm's intensity. The model's ocean comprises a series of one-dimensional columns strung out along the path of the storm. Below a mixed layer of depth h and temperature T_m, there is a temperature jump ΔT, followed by a linear decrease in temperature with depth at a rate Γ (see Fig. 7). The bulk horizontal velocity of the ocean's mixed layer is predicted assuming momentum conservation:

$$\rho_0 \frac{\partial(hu)}{\partial t} = \tau, \tag{5}$$

where ρ_0 is the density of the water and τ is the surface stress generated by the tropical cyclone. The shear instability at the base of the mixed layer is related to the Richardson number (see Emanuel et al. 2004):

$$\mathrm{Ri} = \frac{g\Delta\sigma h}{\sigma u^2}, \tag{6}$$

where $\Delta\sigma = -\alpha\Delta\mathrm{T}$ is the density jump at the base of the mixed layer. Shear instabilities are assumed to maintain the criticality in the Richardson number. Whenever the kinetic energy of the mixed layer is larger than the gravitational potential energy jump below the mixed layer, mixing with underlying water deepens the mixed layer. Enthalpy conservation allows the evaluation of the temperature of the deepened mixed layer. Although here horizontal advection and Coriolis acceleration have been neglected, the model has been shown to reproduce remarkably well the storm intensity obtained when using a fully three-dimensional ocean model (Emanuel et al. 2004).

Schade and Emanuel (1999) have studied the sensitivity of such a model to several oceanic and atmospheric parameters. Here we perform a similar study, focusing on the sensitivity of the maximum velocity attained by tropical cyclone winds to the heat accumulated at the base of the mixed layer. To this aim, we perform a series of numerical simulations in which different atmospheric and oceanic conditions are considered and compute the ratio between the power dissipated and the potential power dissipated by tropical cyclones, $\phi = \mathrm{PD/PPD} = (V_{\max}/V_p)^3$. The evolutions of 1500 tropical cyclones and their dependence on the upper-ocean heat content are studied, under different propagation speeds (between 1 and 10 m s^{-1}) and vertical shear of horizontal winds (wind speed difference between 850 and 200 hPa in the range from 0 to 15 m s^{-1}). We have used many different ocean temperature profiles, obtained by varying: the mixed layer depth from 4 to 160 m, the thermocline slope between 5° and 10°C (100 m)$^{-1}$, and the jump of temperature at the base of the mixed layer between 0.05° and 2°C. The initial surface temperature, set to 27°C, is not varied, as ϕ is remarkably independent of the specific environmental SST, but it is a strong function of the vertical gradients of temperature in the ocean (some tests have been performed with SSTs of 29° and 32°C and show similar results to those presented here). A reference ocean temperature profile (characterized by a mixed layer depth of 28 m and a temperature jump at its base of 1°C) is chosen to define heat anomalies in the ocean model. The upper-ocean heat content anomaly is defined as the heat content in the water column in the top 200 m minus the heat content in the top 200 m of the reference temperature profile. For each of the simulations, the potential intensity and the maximum attained wind speed are used to calculate ϕ. For each set of atmospheric conditions ϕ_0 is defined as the ratio between PD and PPD when the oceanic temperature profile is the reference one, and $\Delta\phi = \phi - \phi_0$.

The results are summarized in Fig. 8. As expected, in general a cold ocean anomaly reduces the attained wind speed, and likewise a warm anomaly increases the value

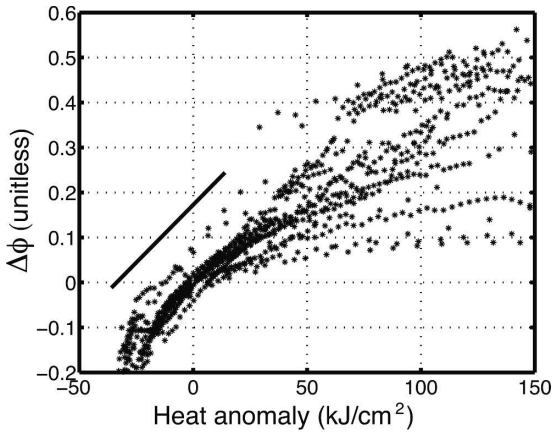

FIG. 8. Relative change of the ratio between power dissipated by tropical cyclones and potential power dissipated, ϕ = PD/PPD, as a function of the upper-ocean heat content anomaly (see text). The solid line has a slope of 0.5 (100 kJ cm^{-2})$^{-1}$.

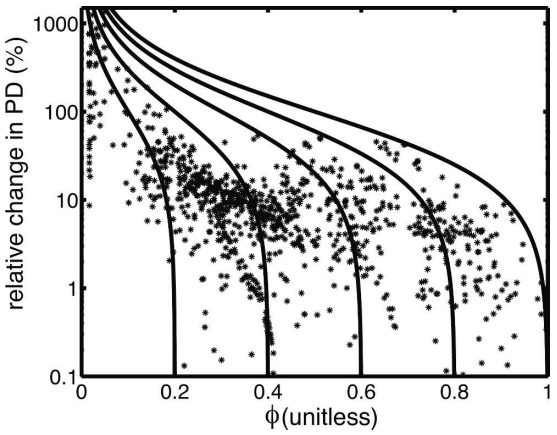

FIG. 9. Relative change in power dissipated by a tropical cyclone when the mixed layer depth is increased by 4 m, as a function of the value of ϕ characterizing them. Each point corresponds to a different set of ocean temperature profiles, propagation speeds, and wind shears. Solid lines indicate the variation required to reach the fraction of PPD indicated by the intersection of each line with the abscissa (the curve on the right is the maximum possible change in PD, corresponding to a tropical cyclone that reaches its PPD).

of ϕ. Points with $\Delta\phi \neq 0$ and null heat anomaly are associated with ocean temperature profiles that differ from the reference value in their mixed layer depth and ΔT but have the same heat content. In these cases the surface cooling owing to entrainment of subsurface water can be different, and thus a small change in ϕ is detected. It is interesting to note that, despite the wide range of parameters used, the dependence of $\Delta\phi$ on the heat anomaly is fairly constant for heat anomalies on the order of a few tens of kilojoules per square centimeter. Its average rate of change is 0.5 (100 kJ cm^{-2})$^{-1}$ of the anomalous warming in the ocean. Considering that values of ϕ_0 for those simulations are in the range 0.12–0.4, this indicates an increase of PD of the order of 60%–200% for a warm anomaly of 50 kJ cm^{-2}. This estimate is in agreement with the observational data that indicate that tropical cyclones undergo strong intensification when passing over warm anomalies on the order of 20–50 kJ cm^{-2} (Goni and Trinanes 2003).

For larger heat anomalies, the response in the value of ϕ depends on the atmospheric characteristics. For example, when a strong wind shear is present, the increase of ϕ with a warming ocean is limited by the fact that the tropical cyclone cannot become intense, as it is limited by atmospheric processes. Another reason for the smaller sensitivity of $\Delta\phi$ to the heat content at large values of the heat anomalies is simply that, as the heat anomaly increases, the value of ϕ gets close to one, and the relative change of ϕ becomes limited by the fact that ϕ cannot grow above one. Tropical cyclones whose intensity is significantly smaller than the potential intensity can clearly intensify more than cyclones whose intensity is already close to their maximum value. This point is quantified in Fig. 9, where the relative change of ϕ is plotted as a function of the initial value of ϕ, when the mixed layer depth is increased by 4 m and no other changes are introduced. Tropical cyclones whose ϕ is 0.2 can double their power dissipated in response to a deepening of the mixed layer of 4 m. The maximum change for a tropical cyclone with $\phi = 0.8$ is about 20%. A relative increase of PD on the order of 50% has been observed for tropical cyclones with $\phi \leq 0.75$.

To summarize, the dependence of ϕ on the heat anomaly ξ is a function that saturates to 1 for large positive anomalies and to 0 for large negative anomalies. We parameterize, for later use, this behavior by using an arctangent function, $\phi = \arctan(a\xi)/\pi + 0.5$. The value of a is chosen to optimally fit the data presented above so that the sensitivity of ϕ to ξ is 0.5 (100 kJ cm^{-2})$^{-1}$ for small ξ (Fig. 10).

Before concluding this section, we want to stress that the sensitivity of PD to a variation in the sea surface temperature below the eye of the tropical cyclone is significantly larger than the sensitivity of PPD to the same variation in the ambient sea surface temperature (see Fig. 11). This effect, studied by Schade (2000), is associated with the energy fluxes at the air–sea interface. The amount of heat that the ocean injects into the atmosphere depends on the horizontal sea surface temperature gradients and not merely on the absolute value of the sea surface temperature. As air in the atmospheric boundary layer moves toward the storm center, its enthalpy increases owing to transfer from the sea. If the sea surface temperature does not have any

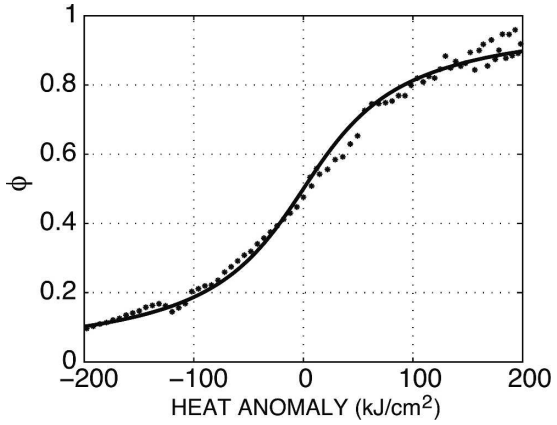

FIG. 10. Ratio between PD and PPD, as function of the heat content anomaly in the upper 150 m of the ocean. To obtain these data the initial mixed layer depth, the temperature jump at the base of the mixed layer, and the thermocline slope have all been varied. The cyclone propagates at 7 m s^{-1} and there is no wind shear. The reference conditions for the ocean are $h = 40$ m, $\Gamma = 8°C\ (100\ m)^{-1}$, and $\Delta T = 0.6°C$, chosen so that the value of ϕ for null heat anomaly is 0.5. Solid line is $\arctan(a\xi)/\pi + 0.5$, with $a = 0.005\pi\ (kJ\ cm^{-2})^{-1}$. The mixed layer depth in these simulations never exceeds 150 m.

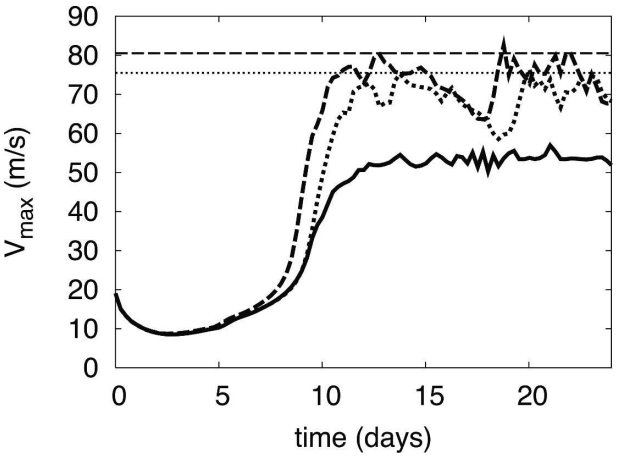

FIG. 11. Maximum wind speed vs time during the evolution of a model tropical cyclone. Thick solid line is for a tropical cyclone interacting with the ocean, with unperturbed SST of 29°C. SST below the eye in this case is 1.7°C lower than the surrounding water, due to entrainment of subsurface water, once the cyclone has reached statistically stationary intensity. Thin solid line is the evolution of the cyclone, were it not causing any surface cooling (in this case the SST is fixed in space and time to 29°C). Dotted line is the evolution of the cyclone intensity developing over an ocean with fixed SST of 27.3°C, i.e., 1.7°C lower than in the previous case. Horizontal lines indicate potential intensity. Note that the maximum wind speed of the cyclone developing over a uniformly cold ocean is significantly larger than the maximum wind speed of the cyclone developing over a warm ocean and creating a cooling below the eye, in spite of the fact that the SST is, in the former case, everywhere colder than or as cold as in the latter case. In these experiments, mixed layer depth is 30 m, temperature jump at the base of the mixed layer is 1°C, thermocline slope is 8°C $(100\ m)^{-1}$, propagation speed of the storm over the ocean is 7 m s^{-1}, and vertical shear of the horizontal large-scale wind is zero.

spatial inhomogeneity, the enthalpy increase is bounded by the (unperturbed) saturation enthalpy of the sea surface. However, if the sea surface temperature is lower below the eyewall, this bounding enthalpy is reduced. A 2.5°C drop in SST is sufficient to prevent any enthalpy increase of the inflowing air, so even a 1°C decrease will significantly weaken the storm.

5. Estimates of feedback magnitude

Here we use the results obtained in the previous sections to estimate the parameters of the simple model of the interplay between upper-ocean heat content and tropical cyclone activity introduced in section 2, Eq. (4). We have shown that the appropriate values for the decay time of anomalous warming in the upper ocean is of the order of 1.4 yr and that the sensitivity of the ratio between PD and PPD to upper-ocean heat anomalies, ξ, can be represented by the function $\phi(\xi) = \arctan(a\xi)/\pi + 0.5$, with $a = 0.005\pi\ (kJ\ cm^{-2})^{-1}$. As for the effect that an anomalous cyclone season has on the upper-ocean heat content, we start from the estimate of mixed layer cooling by tropical cyclone activity for the year 1996 described in Emanuel (2001), then divide it by the surface area affected by tropical cyclones (about $50 \times 10^6\ km^2$), and finally divide the result by 2, based on the observation that, in our MITgcm simulations, the maximum value of the column-integrated heat content anomaly was between one-third and two-thirds of the initial mixed layer cooling. This procedure gives an estimate of $\gamma = 50\ kJ\ cm^{-2}\ yr^{-1}$: a 10% increase in power dissipated by tropical cyclones over a year will result in an anomalous heating of 5 kJ cm^{-2}. The actual increase of heat content after one year will be smaller because of the relaxation to typical conditions that mimics lateral and vertical heat losses over time.

Clearly, the above numbers have to be taken as order of magnitude rather than as exact values, due to the strong approximations and simplifications introduced in the procedures to derive them. For instance, the anomalous mixing introduced in the MITgcm to simulate effects of tropical cyclones does not have the spatial and temporal variability that characterizes tropical cyclones. Another potential source of bias in the estimates comes from the fact that the power dissipated by tropical cyclones depends not only on wind speed, which is the only quantity considered in this study, but also on spatial size and lifetime of cyclones. Moreover,

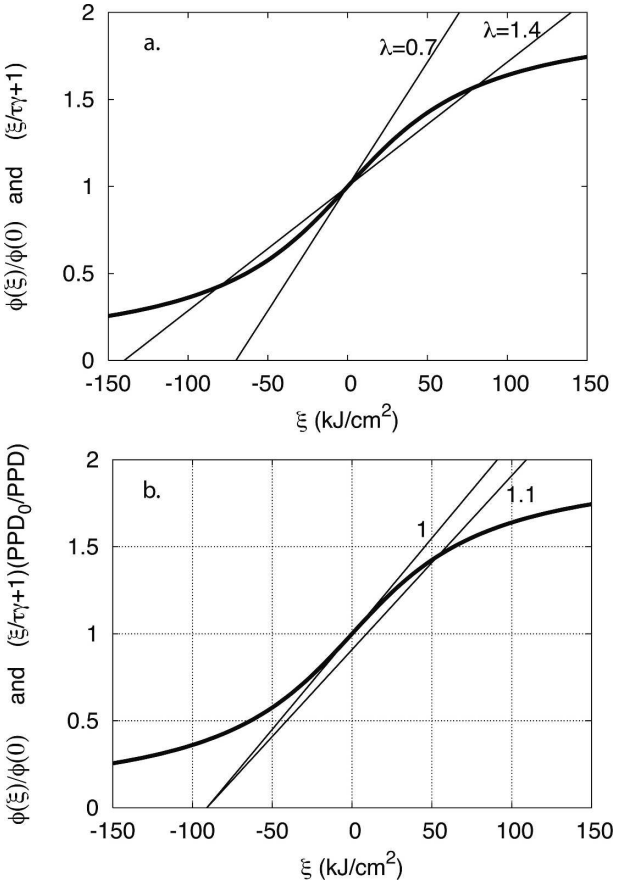

FIG. 12. Graphical analysis of Eq. (4). Steady-state solutions are given by the intersections of $\phi(\xi)/\phi(0)$ with the straight lines. (a) Case PPD = PPD_0. For $\lambda < 1$ the only solution is $\xi = 0$; for $\lambda > 1$ the two external solutions are stable and $\xi = 0$ is unstable. (b) Here the sensitivity of the steady-state solution to an increase of PPD is shown; numbers indicate the value of PPD/PPD_0 for the two different lines. When PPD is increased by 10%, the steady-state value of ϕ, and thus the power dissipated by cyclones, increases by 40%. Here $\lambda = 0.9$.

we choose a function $\phi(\xi)$ so that $\phi(0) = 0.5$: different choices can be made, so the normal value of ϕ in the absence of heat anomalies is anywhere between 0 and 1. For those reasons, in the following we present the behavior of the model for different choices of the parameters.

Steady states of Eq. (4) are given by the solutions of the following equation:

$$\frac{\phi(\xi)}{\phi(0)} = \left(\frac{\xi}{\tau\gamma} + 1\right)\frac{\mathrm{PPD}_0}{\mathrm{PPD}}.$$

As shown in Fig. 12a, depending on the parameter values, there can be one or three steady states. For constant PPD = PPD_0, the solution $\xi = 0$ (normal heat content and normal tropical cyclone activity) becomes

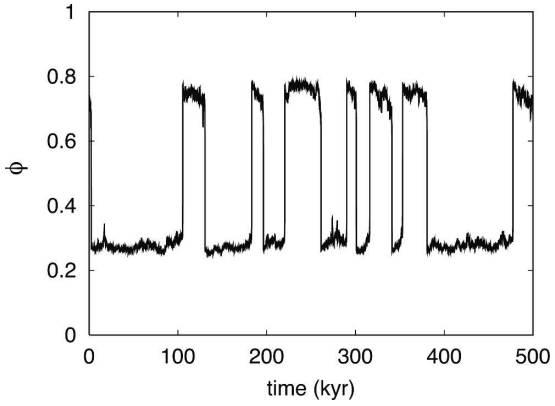

FIG. 13. Ratio between PD and PPD as a function of time, when PPD is a stochastic process with a time scale of 10 000 yr and independent increments with 0.005 standard deviation. Here $\lambda = 1.2$.

linearly unstable when the system goes through a pitchfork bifurcation and two more solutions appear, which happens at

$$\lambda \equiv \frac{\gamma a \tau}{\pi\phi(0)} = 1.$$

It is remarkable that the values of the parameters introduced above lead to $\lambda = 0.7$: a change in τ from 1.4 to 2 yr or the increase of γ from 50 to 80 kJ cm^{-2} yr^{-2} suffices for λ to become supercritical and the present solution to become unstable. The presence of multiple steady states indicates that the interplay between tropical cyclones and upper-ocean heat content can lead to stable solutions representing both weak cyclonic activity (and, consequently, weak ocean mixing and shallow mixed layer) and more vigorous cyclonic activity with deeper mixing and larger heat content in the upper ocean. A relatively small change in the conditions that regulate the interplay between tropical cyclones and upper-ocean mixing could actually induce the transition through the bifurcation, leading to a sudden and large change in the power dissipated by tropical cyclones. For $\lambda > 1$, a small variation in PPD can suffice to allow a transition from the weak to the strong steady state and vice versa. We show in Fig. 13 one such case. Here, PPD is assumed to stochastically vary in time. PPD is defined as an Orstein–Uhlenbeck process (e.g., Gardiner 2004) with decay time of 10 000 yr and Gaussian increments with standard deviation 0.005. The system is perturbed by the stochastic fluctuations in PPD that induce small variations in PD. When the fluctuations are large enough, they induce a transition from one stable steady state to the other one. Time intervals between the transitions are regulated by the characteris-

tics of the stochastic process. Before concluding this brief discussion on multiple steady states, we suggest that they may be relevant for past climate variations (e.g., Eocene warm climate). It is, however, difficult to further explore this issue since we do not know the precise values and sensitivity to ambient conditions of the parameters on which the pitchfork bifurcation at $\lambda = 1$ depends.

We now present the evolution of the tropical cyclone activity when a perturbation in PPD is introduced. This mimics a temporally variable potential intensity owing to modified thermodynamic conditions, such as a small modulation of sea surface temperature. In Fig. 12b the sensitivity of the steady state to a small increase in PPD is shown, for a case with subcritical λ: a 10% increase in PPD is reflected into a four times larger increase in PD. As usual, the specific number is not important, as larger and smaller amplifications can be obtained starting, for instance, from different initial values of $\phi(0)$, but it is significant that large amplification is possible. The temporal evolution of the amplification is shown in Fig. 14a, where a time-varying PPD is considered, $\mathrm{PPD}(t) = \mathrm{PPD}_0(1 + 0.004\ \mathrm{yr}^{-1}\, t)$, corresponding to a 16% increase of PPD in 40 yr. The corresponding increase of the power dissipated by cyclones over the same time interval is 60%. A simulation with a sinusoidal dependence of PPD in time, with a period of 40 yr and amplitude of 5%, is presented in Fig. 14b and shows a similar amplification of the cycle of PD, together with a slight dephasing between the two curves.

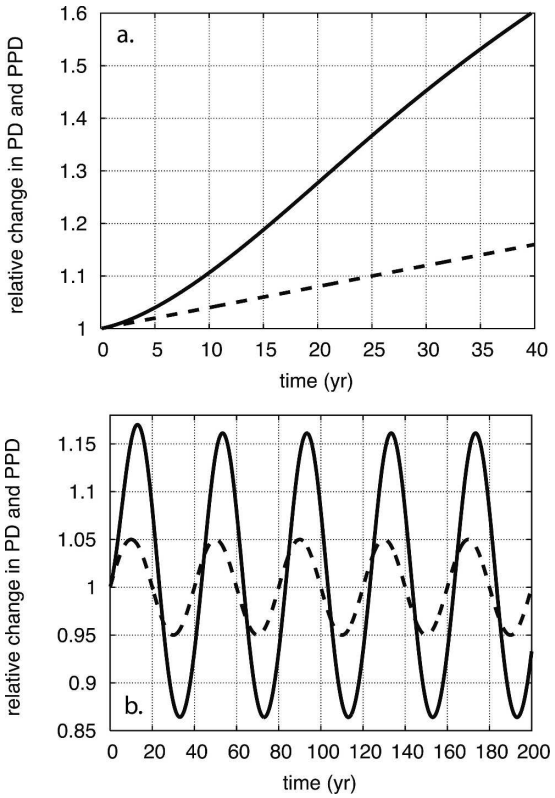

FIG. 14. Evolution of anomalous hurricane dissipated power (solid line) and potential power dissipated (dashed line), normalized by their initial values, from integration of system Eq. (4). (a) PPD is increased by 0.4% of the initial value every year. After 40 yr, PPD has increased by 16% while PD has increased 4 times more; (b) PPD is varied over a period of 40 yr by 10%. The variation of PD is about 3 times larger and delayed by about 3 yr. Here $\phi(0) = 0.5$, $\gamma = 50$, and $\tau = 1.4$ yr.

6. Discussion and conclusions

Potential intensity theory of tropical cyclones (Emanuel 2003) relates maximum attainable wind speed to atmospheric thermodynamic conditions and does not account for ocean interactions. However, it is known that the upper-ocean heat content, even in case of constant sea surface temperature, strongly affects the actual intensity reached by tropical cyclones. Here we have used a simple atmosphere–ocean model to investigate the sensitivity of tropical cyclone intensity to upper-ocean heat content, when the environmental (unperturbed) sea surface temperature is kept constant. The sensitivity manifests through the surface cooling below the eye of the cyclone determined by entrainment of cold water upwelled from underneath. As reported in previous studies (Schade 2000), the sensitivity of cyclone intensity to changes in surface temperature below the eye is much stronger than the sensitivity of potential intensity to environmental sea surface temperature. In turn, sea surface temperature below the eye is affected by the vertical profile of temperature in the ocean, with a deeper initial mixed layer inducing a smaller surface cooling and thus allowing for stronger cyclone intensity. Here, it is shown that in our model the ratio ϕ between the actual power dissipated by a cyclone and the power dissipated by a cyclone that reaches its potential intensity, which is a number between 0 and 1, increases by about 0.1 when the heat content of the upper ocean is increased by 20 kJ cm^{-2} from typical conditions. The rate of change of ϕ with heat content decreases to 0 for both very deep mixed layers (when ϕ saturates to one, in the absence of vertical wind shear) and very shallow mixed layers (when ϕ tends to zero).

There are indications that in the last 50 years the heat content of the upper ocean has increased (Levitus et al. 2005), but the global signal is not statistically significant (Harrison and Carson 2007). For this reason, we focus on the region in the North Atlantic Ocean where tropical cyclones occur (defined as the region where PI $>$ 60

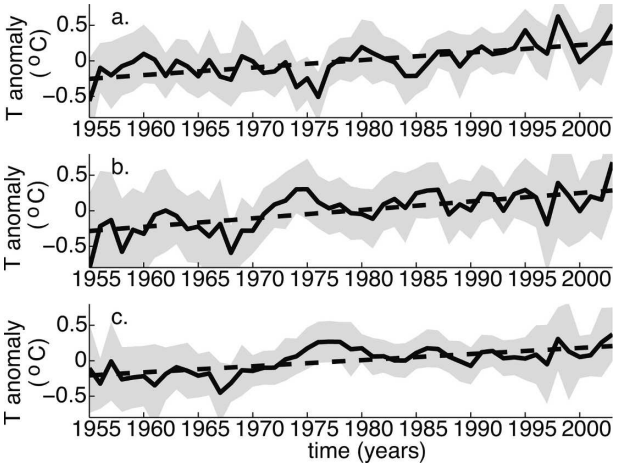

FIG. 15. Temperature anomalies, averaged over the western tropical North Atlantic Ocean at different depths: (a) 50, (b) 150, and (c) 300 m. The dataset is the one presented in Levitus et al. (2005). Shades indicate standard deviations; dashed lines are the linear fits. The null hypothesis of a zero trend can be rejected in all cases at the 95% confidence level.

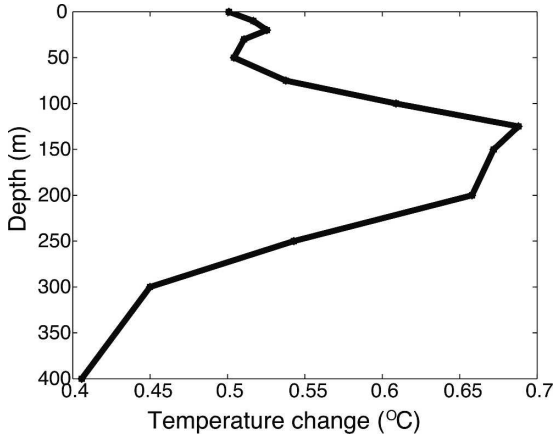

FIG. 16. Mean temperature increase in the last 50 years for the western tropical North Atlantic Ocean. The dataset is the one presented in Levitus et al. (2005). Note that the maximum warming is away from the surface, suggesting a deepening of the mixed layer.

$m\,s^{-1}$, see Fig. 3), that, among the tropical areas of direct relevance for our discussion, has been the best sampled. Large portions of this region show a statistically significant positive trend over the second half of the twentieth century (Harrison and Carson 2007). Positive temperature trends in the upper 700 m over the tropical North Atlantic with PI > 60 m s^{-1} (Fig. 15) are statistically significant at the 95% confidence level and indicate that the largest warming is between 100 and 200 m from the surface, suggesting a deepening of the mixed layer of about 3–4 m over this period. In particular, the data suggest a warming rate at 150 m 35% larger than at the surface (Fig. 16). This causes a reduction of static stability (measured by N^2, where N is the Brunt–Väisälä frequency) of about 6% at 100 m (not shown). Note, however, that the location of the maximum warming below the mixed layer is merely a suggestion and has yet to be proven, as the noise in the data does not allow one to reject the null hypothesis of a uniform warming in the upper 300 m. Previous work reports a warming rate in the North Atlantic of 0.67 W m^{-2} for the period 1955–2005 (Levitus et al. 2005). For comparison, consider that in our model the warming corresponding to an increase of PD of 40% (see Fig. 12b), $\xi = 60$ kJ cm^{-2}, if occurring over 50 years, has a rate of 0.38 W m^{-2}. Although the accuracy of the estimate of ocean warming that occurred over the last few decades still needs to be evaluated, it nevertheless suggests that part of the increase in power dissipated by cyclones (Emanuel 2005) could be related to the increased mixed layer depth.

It is moreover argued that the deepening of the mixed layer could be partially driven by the increased activity of tropical cyclones, which drive stronger and deeper mixing in the ocean. The passages of tropical cyclones and their intense winds induce strong vertical mixing in the upper ocean, followed by a reduction of sea surface temperature mainly due to entrainment of cold water from below. Anomalous air–sea heat fluxes and lateral displacement of water reduce the surface temperature anomaly within a few weeks, while the anomalous warming at the base of the mixed layer owing to the vertical mixing apparently remains in the tropical region for several months. Our ocean general circulation model results suggest that one-third of the warm anomaly in the water column remains in the tropical ocean for more than one year. The anomalous warming created by a particularly intense tropical cyclone season could thus affect the evolution of tropical cyclones in the subsequent season.

The feedback between tropical cyclone activity and upper-ocean heat content has been investigated using a simple model that shows a strong response in power dissipated by tropical cyclones to a small modulation of thermodynamic conditions in the atmosphere and ocean surface. For cyclones with $\phi(0) = 0.5$ it is easy to observe a three- to fourfold amplification of a PPD signal in the dissipated power in this model. Such amplification is smaller for cyclones that initially have a larger value of ϕ and is larger for cyclones that initially have a smaller value of ϕ. It is also shown that the model has a pitchfork bifurcation and that for certain parameter values multiple steady states coexist. This indicates that, in this model, regimes characterized both

by vigorous tropical cyclone activity with strong mixing and large heat content in the upper ocean and weak tropical cyclone activity with weak mixing and small upper-ocean heat content can be sustained. The study has allowed us to estimate the parameter values appropriate to our current conditions to be used in this simple model and has shown that they are fairly close to the bifurcation conditions.

It is interesting to note that the feedback mechanism presented here is potentially relevant for the generation of climate variability. The effect of an intense tropical cyclone season is a warming of the upper ocean and a deepening of the mixed layer in the tropical region. A positive sea surface temperature anomaly in the tropics is associated with a weakening of the trade winds (e.g., Virmani and Weisberg 2006), which affect both the meridional heat transport in the ocean toward higher latitudes (and thus midlatitude temperatures) and Ekman pumping in the subtropical gyres. Since in these regions Ekman pumping creates downwelling, eventually the weakened easterlies drive a shoaling of the thermocline. The presence of two forces that operates in opposing directions (strong cyclones directly forcing the mixed layer to deepen and indirectly reducing Ekman pumping) is an intriguing possible source of climate variability: If a delay between the two forces is present, interannual oscillations would be created.

This study has several limitations. In particular, the evolution of heat anomalies in the ocean general circulation model has not been studied with the spatial and temporal intermittency characteristics appropriate for individual tropical storms. The coarse horizontal resolution that we used allows us to diagnose the displacements of ocean heat anomalies by mean currents and long-wave dynamics but not to study the evolution of a localized strong temperature gradient. In particular, our results might overestimate the warming of the upper ocean following the mixing induced by strong winds because lateral transport of warm surface water into the region of the surface cooling is inhibited by the adopted large-scale structure of the initial anomaly. Under those conditions, sea surface temperature anomalies are mainly eliminated by anomalous air–sea fluxes, rather than by redistribution of heat into the ocean. More refined models are necessary for quantifying the upper-ocean heat content evolution in a more realistic way, as the general circulation model that we used does not resolve mesoscale and submesoscale features that play an important role in the restratification of the mixed layer (Boccaletti et al. 2007; Oschlies 2002). Parameterizations of such processes into large-scale models are currently being developed (e.g., Ferrari and McWilliams 2007, manuscript submitted to *Ocean Modell.*). Moreover, we have not included direct effects on ϕ of vertical shear of horizontal winds, which is known to strongly limit intensity of tropical cyclones, but probably not their variability on long times (Hoyos et al. 2006). Also, sensitivity of tropical cyclone lifetime to ocean characteristics has not been included. Nevertheless, we believe that the presented feedback mechanism deserves further exploration, both using observational data of the upper-ocean heat content before and after the passage of cyclones and by theoretical and numerical investigation of the evolution of the temperature profiles in the ocean for long times after the passage of a tropical cyclone.

Acknowledgments. We are grateful to A. Sobel and to two anonymous reviewers for their comments on an earlier version of the manuscript.

REFERENCES

Bender, M., and I. Ginis, 2000: Real-case simulations of hurricane–ocean interaction using a high-resolution coupled model: Effects on hurricane intensity. *Mon. Wea. Rev.,* **128,** 917–946.

——, ——, and Y. Kurihara, 1993: Numerical simulations of tropical cyclone-ocean interaction with a high-resolution coupled model. *J. Geophys. Res.,* **98,** 23 245–23 263.

Bister, M., and K. Emanuel, 2002: Low frequency variability of tropical cyclone potential intensity 1. Interannual to interdecadal variability. *J. Geophys. Res.,* **107,** 4801, doi:10.1029/2001JD000776.

Boccaletti, G., R. Ferrari, and B. Fox-Kemper, 2007: Mixed layer instabilities and restratification. *J. Phys. Oceanogr.,* **37,** 2228–2250.

Boos, W., J. Scott, and K. Emanuel, 2004: Transient diapycnal mixing and the meridional overturning circulation. *J. Phys. Oceanogr.,* **34,** 334–341.

Cione, J., and E. Uhlhorn, 2003: Sea surface temperature variability in hurricanes: Implications with respect to intensity change. *Mon. Wea. Rev.,* **131,** 1783–1796.

Conkright, M., R. Locarnini, H. Garcia, O. Brien, T. Boyer, C. Stephens, and J. Antonov, 2002: *World Ocean Atlas 2001: Objective Analyses, Data Statistics, and Figures.* National Oceanographic Data Center, CD-ROM Documentation, 17 pp.

D'Asaro, E., 2003: The ocean boundary layer below Hurricane Dennis. *J. Phys. Oceanogr.,* **33,** 561–579.

——, and C. McNeil, 2007: Air-sea gas exchange at extreme wind speeds measured by autonomous oceanographic floats. *J. Mar. Syst.,* **66,** 92–109.

Elsner, J., A. Tsonis, and T. Jagger, 2006: High-frequency variability in hurricane power dissipation and its relationship to global temperature. *Bull. Amer. Meteor. Soc.,* **87,** 763–768.

Emanuel, K., 1987: The dependence of hurricane intensity on climate. *Nature,* **326,** 483–485.

——, 1995: The behavior of a simple hurricane model using a convective scheme based on subcloud-layer entropy equilibrium. *J. Atmos. Sci.,* **52,** 3960–3968.

——, 1999: Thermodynamic control of hurricane intensity. *Nature,* **401,** 665–669.

——, 2000: A statistical analysis of tropical cyclone intensity. *Mon. Wea. Rev.,* **128,** 1139–1152.

——, 2001: Contribution of tropical cyclones to meridional heat transport by the oceans. *J. Geophys. Res.,* **106** (D14), 14 771–14 781.

——, 2003: Tropical cyclones. *Annu. Rev. Earth Planet. Sci.,* **31,** 75–104.

——, 2005: Increasing destructiveness of tropical cyclones over the past 30 years. *Nature,* **436,** 686–688.

——, 2007: Comment on "Sea-surface temperatures and tropical cyclones in the Atlantic basin" by Patrick J. Michaels, Paul C. Knappenberger, and Robert E. Davis. *Geophys. Res. Lett.,* **34,** L06702, doi:10.1029/2006GL026942.

——, C. D. Autels, C. Holloway, and R. Korty, 2004: Environmental control of tropical cyclone intensity. *J. Atmos. Sci.,* **61,** 843–858.

Ferrari, R., J. C. McWilliams, V. M. Canuto, and M. Dubovikov, 2008: Parameterization of eddy fluxes near oceanic boundaries. *J. Climate,* in press.

Gardiner, C., 2004: *Handbook of Stochastic Methods for Physics, Chemistry, and the Natural Sciences.* 3rd ed. Springer-Verlag, 415 pp.

Goni, G., and J. Trinanes, 2003: Ocean thermal structure monitoring could aid in the intensity forecast of tropical cyclones. *Eos, Trans. Amer. Geophys. Union,* **84,** 573–580.

Harrison, D., and M. Carson, 2007: Is the World Ocean warming? Upper-ocean temperature trends: 1950–2000. *J. Phys. Oceanogr.,* **37,** 174–187.

Hoyos, C., P. Agudelo, P. Webster, and J. Curry, 2006: Deconvolution of the factors contributing to the increase in global hurricane intensity. *Science,* **312,** 94–97.

Knutson, T., and R. Tuleya, 2004: Impact of CO_2-induced warming on simulated hurricane intensity and precipitation: Sensitivity to the choice of climate model and convective parameterization. *J. Climate,* **17,** 3477–3495.

——, ——, W. Shen, and I. Ginis, 2001: Impact of CO_2-induced warming on hurricane intensities as simulated in a hurricane model with ocean coupling. *J. Climate,* **14,** 2458–2468.

Levitus, S., J. Antonov, and T. Boyer, 2005: Warming of the world ocean, 1955–2003. *Geophys. Res. Lett.,* **32,** L02604, doi:10.1029/2004GL021592.

Lin, I.-I., C.-C. Wu, K. Emanuel, I.-H. Lee, C.-R. Wu, and I.-F. Pun, 2005: The interaction of Supertyphoon Maemi (2003) with a warm ocean eddy. *Mon. Wea. Rev.,* **133,** 2635–2649.

Marshall, J., A. Adcroft, C. Hill, L. Perelman, and C. Heisey, 1997: A finite-volume, incompressible Navier Stokes model for studies of the ocean on parallel computers. *J. Geophys. Res.,* **102,** 5753–5766.

Michaels, P., P. Knappenberger, and R. Davis, 2006: Sea-surface temperatures and tropical cyclones in the Atlantic basin. *Geophys. Res. Lett.,* **33,** L09708, doi:10.1029/2006GL025757.

Oschlies, A., 2002: Improved representation of upper-ocean dynamics and mixed layer depths in a model of the North Atlantic on switching from eddy-permitting to eddy-resolving grid resolution. *J. Phys. Oceanogr.,* **32,** 2277–2298.

Persing, J., and M. Montgomery, 2003: Hurricane superintensity. *J. Atmos. Sci.,* **60,** 2349–2371.

Price, J., 1981: Upper ocean response to a hurricane. *J. Phys. Oceanogr.,* **11,** 153–175.

Schade, L., 2000: Tropical cyclone intensity and sea surface temperature. *J. Atmos. Sci.,* **57,** 3122–3130.

——, and K. Emanuel, 1999: The ocean's effect on the intensity of tropical cyclones: Results from a simple coupled atmospheric–ocean model. *J. Atmos. Sci.,* **56,** 642–651.

Scott, J., and J. Marotzke, 2002: The location of diapycnal mixing and the meridional overturning circulation. *J. Phys. Oceanogr.,* **32,** 3578–3595.

Shay, L., G. Goni, and P. Black, 2000: Effects of a warm oceanic feature on Hurricane Opal. *Mon. Wea. Rev.,* **128,** 1366–1383.

Virmani, J., and R. Weisberg, 2006: The 2005 hurricane season: An echo of the past or a harbinger of the future? *Geophys. Res. Lett.,* **33,** L05707, doi:10.1029/2005GL025517.

Zhu, T., and D.-L. Zhang, 2006: The impact of the storm-induced SST cooling on hurricane intensity. *Adv. Atmos. Sci.,* **23,** 14–22.